Journal of Virology

Small Rho GTPases and Cholesterol Biosynthetic Pathway Intermediates in African Swine Fever Virus Infection

Jose I. Quetglas, Bruno Hernáez, Inmaculada Galindo, Raquel Muñoz-Moreno, Miguel A. Cuesta-Geijo and Covadonga Alonso

J. Virol. **2012, 86(3):1758. DOI: 10.1128/JVI.05666-11.**
Published Ahead of Print 23 November 2011.

JVI Journals.ASM.org

Small Rho GTPases and Cholesterol Biosynthetic Pathway Intermediates in African Swine Fever Virus Infection

Jose I. Quetglas,* Bruno Hernáez, Inmaculada Galindo, Raquel Muñoz-Moreno, Miguel A. Cuesta-Geijo, and Covadonga Alonso

Departamento de Biotecnología–Instituto Nacional de Investigación y Tecnología Agraria y Alimentaria, INIA, Madrid, Spain

The integrity of the cholesterol biosynthesis pathway is required for efficient African swine fever virus (ASFV) infection. Incorporation of prenyl groups into Rho GTPases plays a key role in several stages of ASFV infection, since both geranylgeranyl and farnesyl pyrophosphates are required at different infection steps. We found that Rho GTPase inhibition impaired virus morphogenesis and resulted in an abnormal viral factory size with the accumulation of envelope precursors and immature virions. Furthermore, abundant defective virions reached the plasma membrane, and filopodia formation in exocytosis was abrogated. Rac1 was activated at early ASFV infection stages, coincident with microtubule acetylation, a process that stabilizes microtubules for virus transport. Rac1 inhibition did not affect the viral entry step itself but impaired subsequent virus production. We found that specific Rac1 inhibition impaired viral induced microtubule acetylation and viral intracellular transport. These findings highlight that viral infection is the result of a carefully orchestrated modulation of Rho family GTPase activity within the host cell; this modulation results critical for virus morphogenesis and in turn, triggers cytoskeleton remodeling, such as microtubule stabilization for viral transport during early infection.

The members of Rho family of small GTPases are essential key regulators of diverse critical cellular functions, including cytoskeleton dynamics, cell cycle progression, migration, the generation of reactive oxygen species, and gene expression (16, 29, 35, 53). Like the majority of Ras superfamily proteins, most Rho GTPases function as molecular switches and cycle between an active GTP-bound form and an inactive GDP-bound one. Two types of regulatory proteins control this cycling: guanine nucleotide exchange factors (GEFs) that promote activation of these proteins during signal transduction by exchanging of GDP for GTP molecules and, in contrast, GTPase-activating proteins (GAPs) that promote the hydrolysis of the bound GTP molecules, thus allowing the transfer of the GTPase back to the inactive state (7, 9). In addition, Rho GTPases must often undergo posttranslational prenylation to become functionally active (43). Thus, their localization, insertion into membranes, and protein-protein interactions require covalent incorporation into the carboxy terminus of either farnesyl pyrophosphate (FPP) or geranylgeranyl pyrophosphate (GGPP) (62). Since these prenyl groups are derived from mevalonic acid, which is also the starting material for the cholesterol biosynthesis, statins have been widely used to inhibit the prenylation of Ras-related proteins, particularly the Rho GTPase subfamily (24, 28, 41).

Given the control that the most studied Rho GTPase members (RhoA, Rac1, and Cdc42) exert over cytoskeleton dynamics, vesicle trafficking, and signaling pathways, it has been hypothesized that they make a major contribution to viral entry, replication, and morphogenesis. In this regard, Rac1/Cdc42 regulates actin dynamics and architecture during macropinocytotic entry of diverse large DNA viruses, such as vaccinia virus (42, 45) and adenovirus (40). In addition, during entry into host cells, herpes simplex virus 1 (HSV-1) activates Rac1 and Cdc42, which results in the induction of filopodia and lamellipodia in epithelial cells and fibroblasts (33). Rho GTPases are also implicated in microtubule regulation during capsid trafficking of Kaposi's sarcoma-associated herpesvirus (48). Recently, it has been shown that vaccinia virus F11L protein interacts directly with RhoA to inhibit its downstream signaling (61). This F11L-mediated inhibition of RhoA signaling has been proposed to be required for an efficient virus release from infected cells (4) and also for stimulating virus-induced cell motility (4, 12, 66) and the spreading of infection. RhoA signaling is required for respiratory syncytial virus replication and morphogenesis (26). Moreover, the expression of active Rac1 is increased after hepatitis B virus replication (59).

African swine fever virus (ASFV) is the causative agent of a severe and highly lethal hemorrhagic disease that affects domestic pigs. This large icosahedral and enveloped DNA virus is the only known member of the family *Asfarviridae* (17). It enters host cells by clathrin- and dynamin-dependent endocytosis after attachment to a still unknown cell receptor(s) and requires later fusion between the viral envelope and endosome membrane to deliver DNA into cytoplasm (31, 60). This fusion event requires the characteristic acidic pH of the endosomal environment and also the presence of cholesterol at the plasma membrane of the target cell (6, 22). Like many other viruses, during the early stages of infection ASFV interacts with the microtubule cytoskeleton and requires retrograde dynein-based transport to constitute the perinuclear virus factory (3, 30), where DNA replication and assembly occur. This specialized site, close to the microtubule organizing center, contains mostly viral DNA, most of the viral proteins, immature and mature virions, and also abundant virus-induced membranes. Microtubule motors have also been proposed to be involved in at least three other events that occur in the ASFV replication cycle, namely, vimentin rearrangement into a cage that

Received 13 July 2011 **Accepted** 8 November 2011

Published ahead of print 23 November 2011

Address correspondence to C. Alonso, calonso@inia.es.

* Present address: Division of Gene Therapy, School of Medicine, Center for Applied Medical Research, University of Navarra, Pamplona, Spain.

doi:10.1128/JVI.05666-11

finally surrounds the viral factory (57), the recruitment of virus-targeted membranes to the virus factory (54), and the transport of fully assembled virions to the plasma membrane before their release from an infected cell by budding (36).

Here we explored, for the first time, the relevance of the Rho GTPase subfamily during ASFV infection. We found that a general inhibition of Rho GTPases leads to a decrease in viral yields and deficient viral morphogenesis. Most importantly, since Rac1 resulted activated early during infection and coincident with an increase in microtubule acetylation, the data obtained suggest the involvement of Rac1-mediated signaling on ASFV intracellular transport.

MATERIALS AND METHODS

Cell culture, viruses, and plasmids. Vero cells were obtained from the European Collection of Cell Cultures (ECACC) and maintained in Dulbecco modified Eagle medium supplemented with 5% fetal bovine serum at 37°C and 5% CO_2. The tissue culture-adapted ASFV strain BA71V was used in all experiments (18). Where indicated, a recombinant virus expressing viral protein p54 fused to the green fluorescence protein (GFP) was used (B54GFP-2 [32]) to identify viral factories by confocal microscopy. Cell infections and titrations were carried out as previously described. When indicated, we used highly purified ASFV as described elsewhere (10).

Plasmids (pcDNA3) encoding wild-type (wt), dominant-negative (17N), and constitutively active (Q61L) forms of Rac1 fused to GFP were kindly provided by Ole Gjoerup (58). Constructs expressing the glutathione *S*-transferase (GST)-Rac1/Cdc42 binding domain of Pak1 (GST-PBD) were a generous gift from Keith Burridge (5). Transient expression in Vero cells was achieved by transfection using Fugene HD transfection reagent (Roche) and 2 μg of DNA/10^6 cells (ratio 1:6) according to the manufacturer's instructions.

Antibodies and other reagents. Antibodies against Cdc42 and Rac1 were obtained from BD Transduction Laboratories. Monoclonal antibodies against α-tubulin and acetylated α-tubulin were purchased from Sigma. Jose M. Escribano provided the monoclonal antibody against p30. The monoclonal antibody against p72 clone 18BG3 was purchased from Ingenasa. Rabbit polyclonal serum against ASFV protein pE120R was obtained after immunization with recombinant protein. Anti-rabbit and anti-mouse antibodies conjugated to horseradish peroxidase were purchased from GE Healthcare. Alexa Fluor 488- and Alexa Fluor 594-conjugated anti-mouse IgG antibodies were from Molecular Probes.

Triton X-100, lovastatin (Mevinolin), farnesyl pyrophosphate (FPP), geranylgeranyl pyrophosphate (GGPP), L-mevalonate, cholesterol, β-actin polyclonal antibody, and Hoechst 33258 were purchased from Sigma. *Clostridium difficile* toxin B (CdTB), FTI-277 (farnesyltransferase inhibitor [FTase] inhibitor), GGTI-286 (geranylgeranyltransferase inhibitor [GGTI]), NSC23766 (Rac1 inhibitor), and Fluorsave were obtained from Calbiochem.

Cytotoxicity assay. The cytotoxicity elicited by inhibitors was analyzed by using a lactate dehydrogenase cytotoxicity assay kit (Promega) and by trypan blue exclusion.

Drug treatments and infections. Vero cells were treated with a range of concentrations (1 to 3 μM) of lovastatin (Lov) for 24 or 48 h at 37°C. Add-back of intermediate metabolites was done at the following concentrations: 200 μM mevalonate (Mev), 5 μM GGPP, 5 μM FPP, or 5 μg of cholesterol/ml, together with 1 to 3 μM Lov. In all cases, at 24 h after ASFV infection (BA71V isolate, 0.5 PFU/cell), cells and supernatants were collected to determine virus progeny production by plaque assay, as previously described (25). In a second set of experiments, the cells were incubated with a range of concentrations of GGTI-286 (10 to 30 μM), FTI-277 (10 to 30 μM), or CdTB (25 to 100 ng/ml). These chemical inhibitors were added either 2 h before virus inoculation and removed after viral adsorption or maintained throughout infection, or they were added at 3 h postinfection (hpi) and maintained until the end of the experiment. In order to evaluate the infectivity of ASFV in the presence of these drugs, we infected pretreated cells (2 h before virus inoculation for GGTI-286, FTI-277, or CdTB or 24 and 48 h before virus inoculation when using Lov) and analyzed the number of infected cells at 3 hpi by immunofluorescence detection of viral early protein p30 (see the discussion of immunofluorescence analysis). Where indicated, cells were infected at high multiplicity of infection (MOI), i.e., ~20 PFU/cell.

GTPase activation assays. Serum-starved Vero cells (60% confluence), infected or mock infected with ASFV at an MOI of 5 PFU/cell, were washed with phosphate-buffered saline (PBS) at a range of times postinfection and lysed in a buffer containing 10% glycerol, 50 mM Tris-HCl (pH 7.4), 100 mM NaCl, 1% NP-40, 2 mM $MgCl_2$, and protease inhibitors.

Bacterially expressed and purified GST-PBD (p21-binding domain of Pak1) interacts with activated GTP-bound Rac1 and Cdc42 was used to pull-down GTP-bound forms of Rac1 and Cdc42, as described previously (15, 55). Equal amounts of total protein from cell lysates were incubated for 1 h at 4°C with glutathione-Sepharose 4B beads (GE Healthcare) previously conjugated to GST-PBD. After extensive washing, bound proteins were analyzed by Western blotting with monoclonal antibodies against Rac1 or Cdc42. Previously, lysates were probed with the same antibodies to detect total Rac1 and Cdc42 in the samples. To determine the levels of active GTPases, the intensities of the corresponding bands were measured by densitometry (Tina 2.0) and normalized to values obtained with mock-infected cells.

RhoA, Rac1, and Cdc42 activation was also measured using RhoA-, Rac1-, and Cdc42-specific G-Lisa activation kits (Cytoskeleton, Inc.) according to the manufacturer's instructions. Briefly, Vero cells were seeded in 25-cm^2 flasks for the indicated confluence and serum starved for 24 h prior to BA71V infection (5 PFU/cell). Mock-infected and infected cells were harvested in lysis buffer at the indicated times postinfection. G-Lisa kits used 96-well plates coated with the binding domain of the corresponding GTPase effector protein. GTPase-GDP was removed during washing steps, and GTPase-GTP was detected with specific antibodies, followed by absorbance at 490 nm.

Detection and quantitation of the ASFV genome. DNA from infected or mock-infected Vero cells with ASFV 0.5 PFU/cell was extracted and purified with a DNeasy blood and tissue kit (Qiagen) at 16 hpi. Detection and quantitation of the ASFV genome was achieved by quantitative real-time PCR using specific oligonucleotides and a TaqMan probe, as previously described (38). The amplification reaction was performed in a Rotor-Gene RG3000 (Corbett Research) as follows: 1 cycle at 94°C for 10 min, then 45 cycles at 94°C for 15 s, and finally 45 cycles at 58°C for 1 min. Positive and negative amplification controls (DNA purified from ASFV virions and DNA from mock-infected cells, respectively) were included in the assay, and duplicates from each sample were analyzed.

Western blot analysis. After estimation of total protein in samples by the Bradford method, 30 μg of protein was resolved by SDS-PAGE and transferred to nitrocellulose membranes (Bio-Rad). Membranes were probed for 1 h at room temperature with the corresponding primary antibodies in PBS containing 0.05% Tween 20 (PBS-T; Sigma) at the following dilutions: monoclonal antibody against p30 (1:500), monoclonal antibody anti-p72 (1:5000), mouse monoclonal antibody anti-Rac1 (1:1,000), mouse monoclonal antibody anti-Cdc42 (1:250), mouse monoclonal antibodies anti-α-tubulin (1:4,000), and anti-acetylated α-tubulin (1:2,000). As a protein loading control, we included the detection of actin with polyclonal rabbit anti-β-actin serum diluted 1:250. After an extensive washing with PBS-T, membranes were incubated with anti-mouse IgG antibody (1:5,000) or anti-rabbit IgG (1:4,000), both conjugated to horseradish peroxidase. Finally, bands were developed by using an enhanced chemiluminescence reaction with a Western blot detection reagent (GE Healthcare).

Immunofluorescence analysis. Vero cells (60% confluence) were grown on glass coverslips and then infected with BA71V or B54GFP-2. In

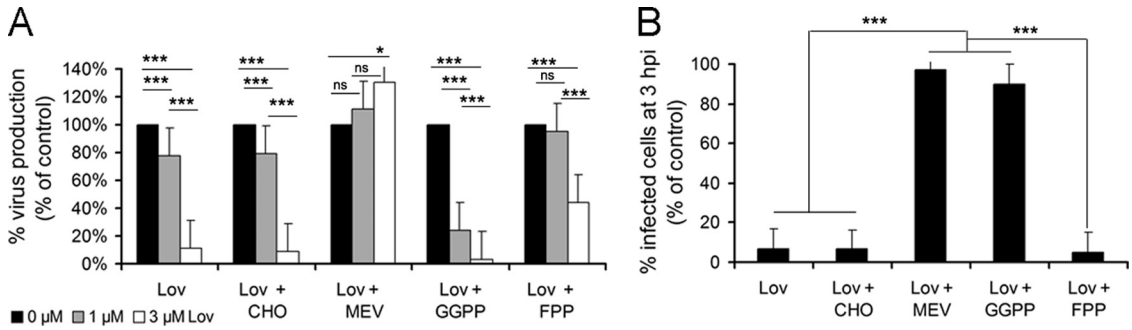

FIG 1 Antiviral effect of lovastatin on ASFV infection. Vero cells were incubated with increasing, but nontoxic, concentrations of lovastatin for 24 h before ASFV infection (0.5 PFU/cell). Where indicated, mevalonate (Mev), cholesterol (CHO), FPP, or GGPP was added to cells. (A) Virus progeny at 24 hpi was analyzed by plaque assay, and virus yields are represented as a percentage of the untreated control cells. (B) Similarly, the number of infected cells (infectivity) at 3 hpi was determined by immunofluorescence in Vero cells treated with 3 μM lovastatin and are represented as a percentage of untreated infected cells. Means and SD correspond to three independent experiments. Values that are significantly different from each other are indicated (***, $P < 0.001$;*, $P < 0.05$).

infectivity assays, at 3 hpi, the cells were rinsed with PBS, fixed with PBS–3.8% paraformaldehyde for 10 min, and permeabilized with 0.2% PBS–Triton X-100 for 15 min. Infected cells at this time were identified by detection of early ASFV protein with monoclonal anti-p30 antibody (1:200). For the viral factory analysis, cells infected with B54GFP-2 were fixed at 16 hpi. Internalized virions in pCDNA-3-transfected cells were detected at 1 hpi with monoclonal antiviral major capsid protein p72 (1:1,000). Rabbit polyclonal serum against pE120R was diluted 1:500. The secondary antibodies used were an anti-mouse IgG antibody conjugated to either Alexa Fluor 488 or Alexa Fluor 549. Nuclei and also DNA in virus factories were identified by staining with Hoechst 33258. Finally, coverslips were mounted onto slides using Fluorsave reagent.

Confocal microscopy was carried out in a Leica confocal microscope TCS SP2-AOBS equipped with ×63 and ×100 objective lenses. The digital images were processed with Adobe Photoshop 8.0.

Electron microscopy. For conventional Epon section analysis, Vero cells, preincubated or not with toxin B, were infected with ASFV at 1 PFU/cell and fixed at 16 hpi with 2.5% glutaraldehyde (Sigma) in PBS for 30 min at room temperature. Postfixation was carried out with 1% OsO_4 in PBS at room temperature for 90 min. The samples were then dehydrated with acetone and embedded in Epon according to standard procedures. Samples were examined at 80 kV in a JEOL JEM 10-10 electron microscope. The digital images were processed with Adobe Photoshop 8.0.

Statistical analysis. All error terms are expressed as standard deviations (SD). Prism software (GraphPad Software, Inc., San Diego, CA) was used for the statistical analysis. A one-way analysis of variance test, followed by Bonferroni's multiple-comparison test, was used to compare different experimental groups. *P* values of <0.05 were considered statistically significant.

RESULTS

ASFV infection requires host protein prenylation at several stages of the infectious cell cycle. To study the relevance of the cholesterol biosynthesis pathway and its precursors during ASFV infection, we used lovastatin (Lov), a powerful inhibitor of 3-hydroxy-3-methylglutaryl-coenzyme A (HMG-CoA) reductase, the enzyme that catabolizes the conversion of HMG-CoA to mevalonate (Mev). Vero cells were incubated with nontoxic concentrations of Lov for 24 or 48 h prior to ASFV infection. Under these conditions, we first analyzed virus production at 24 h postinfection (hpi) by plaque assay. A dramatic reduction of virus progeny was observed in a dose-dependent manner after 24 h of incubation with Lov (Fig. 1A). The addition of the immediate precursor Mev to Lov-treated cells resulted in the recovery of viral yields to reach values similar to those obtained with untreated control cells. This effect was not detected when other intermediate precursors of the cholesterol biosynthesis pathway, such as the isoprenoids GGPP and FPP, were added. Neither was this effect observed with cholesterol add-back. In order to determine whether this reduction in virus progeny correlated with a decrease in ASFV infectivity after Lov treatment, we counted the number of infected cells as early as 3 hpi by indirect immunofluorescence. Lov caused a severe reduction in the number of infected cells (ca. 85%) compared to untreated controls. The effect of Lov on ASFV infectivity was reversed by complementation with Mev or GGPP, but not by the single addition of FPP or cholesterol add-back (Fig. 1B). Similar results were obtained in cells incubated with Lov for 48 hpi (data not shown).

These results indicate a relevant role for cholesterol pathway intermediates and prenyl groups (GGPP and FPP) in posttranslational protein modification during the first stages of ASFV infection. Thus, we evaluated the effect of specific inhibitors of geranylgeranyl transferase I (GGTI-286) and farnesyltransferase I (FTI-277) at various steps of ASFV infection (see Materials and Methods). Inhibition with GGTI-286 resulted in a decrease in the number of infected cells at 3 hpi, which correlated with defective virus production levels independently of the time point at which the inhibitor was added (Fig. 2). These observations are consistent with results from Lov experiments and suggest a role for geranylgeranylation during the first stages of infection, including viral entry. In addition, the reduction of viral yields observed after inhibition of geranylgeranylation with GGTI-286 correlated with a reduction in ASFV DNA replication, as shown by quantitative PCR (Fig. 2C). However, incubation with FTI-277 did not impair ASFV infectivity or virus production when it was added to cells at 3 hpi (Fig. 2). This finding indicates that efficient infection requires farnesylation during the first stages of infection but not after the viral entry into the host cell.

Downregulation of Rho GTPases by toxin B affects ASFV infection but not cell infectivity. Geranylgeranylation promotes activation of many members of the Rho GTPase family that participate in a range of cellular processes, including viral entry into host cells (14, 42, 48). Our data show that geranylgeranylation is relevant during ASFV infection. We thus examined whether Rho GTPases participate in ASFV infection. To this end, we used toxin B from *Clostridium difficile* (CdTB) as a specific inhibitor that

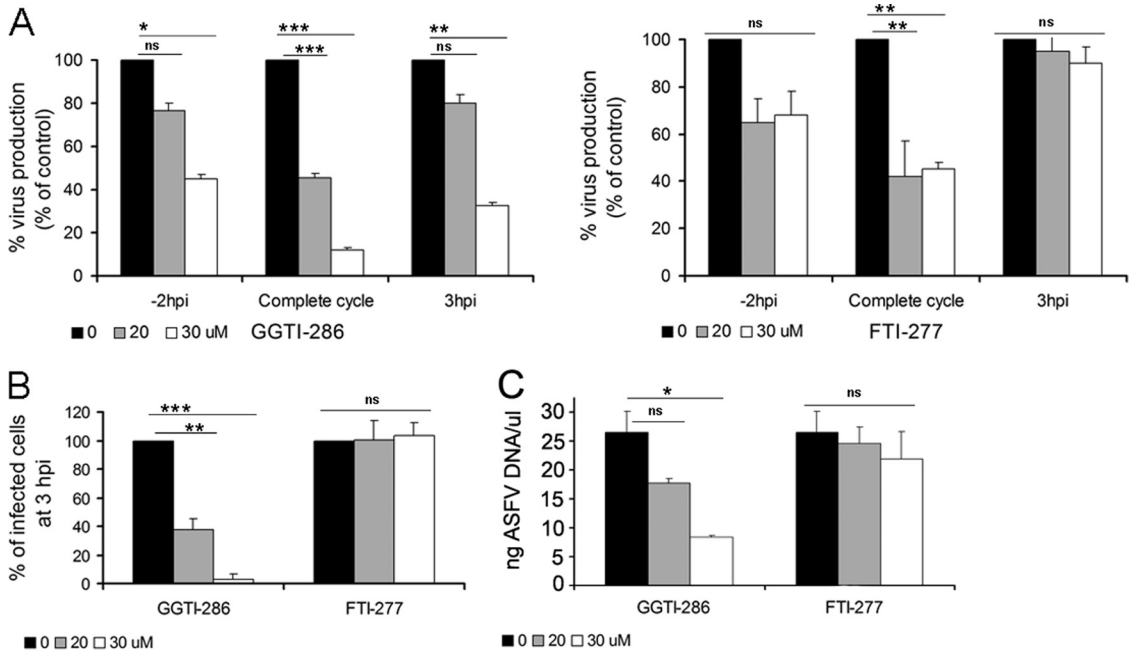

FIG 2 ASFV infection in the presence of prenylation inhibitors. (A) Virus progeny from ASFV-infected cells in the presence of geranylgeranyltransferase I specific inhibitor (GGTI-286) or farnesyltransferase specific inhibitor (FTI-277) at 24 hpi was determined by plaque assay. Inhibitors were added to cells 2 h prior to infection (−2 hpi) or 3 h postinfection (3 hpi) or were present throughout infection. (B) The number of infected cells at 3 hpi in the presence of increasing concentrations of GGTI-286 or FTI-277 was also determined as described previously. (C) ASFV DNA replication at 16 hpi after treatment with increasing concentrations of inhibitors GGTI-286 and FT-277 was analyzed by quantitative PCR. The means and SD correspond to three independent experiments. Values that are significantly different from each other are indicated (***, $P < 0.001$; **, $P < 0.01$; *, $P < 0.05$).

efficiently blocks the interaction of these GTPases with their effectors, resulting in functionally inactive GTPases. The addition of CdTB resulted in rapid depletion of actin stress fibers in Vero cells, which is indicative of successful inhibition of Rho GTPases (data not shown). The incubation of Vero cells with CdTB significantly reduced (ca. 60%) virus titers at 24 hpi compared to untreated cells (Fig. 3A). This effect was detected only when the inhibitor was added to cells before virus inoculation, with no significant differences between removing the inhibitor after virus adsorption and maintaining it throughout the infection. This result raised the question as to whether Rho GTPases contribute to ASFV entry. To study this possibility, we analyzed virus infectivity, as the ratio of infected versus noninfected cells, at 3 hpi in CdTB-treated cells, and we did not find differences in the number of infected cells after CdTB treatment compared to untreated control cells (Fig. 3B). Moreover, we confirmed that viral entry was not affected by the inactivation of Rho GTPases, as shown by the synthesis rates of early (p30) and late (p72) viral proteins detected by immunoblotting of cell lysates at different times of infection, and we did not find significant differences between CdTB treated and untreated cells (Fig. 3C).

ASFV infectivity was not affected by the downregulation of Rho GTPases, thus raising the possibility that the impairment of viral morphogenesis explains the reduction of viral yields observed after CdTB treatment. We next analyzed whether early Rho GTPase inactivation affected the ASFV morphogenesis that takes place at perinuclear viral factories. Vero cells were incubated or not incubated with CdTB, which was removed after virus adsorption. Viral factories were then examined at 16 hpi by confocal microscopy. To identify and analyze these factories, cells were infected with B54GFP-2, a recombinant ASFV expressing enhanced GFP (EGFP) fused to viral protein p54. Cells infected in the presence of CdTB exhibited loose and less compact viral factories (Fig. 3D), and this appearance correlated with larger dimensions (average diameter of 5.56 ± 1.68 μm) than those in nontreated infected cells (average diameter of 4.01 ± 1.25 μm). This observation suggests that an inadequate constitution of the viral assembly site or an incorrect assembly of newly generated virions after Rho GTPase inactivation caused the reduction in viral yields observed after CdTB treatment. In order to confirm this hypothesis, we examined in more detail the effects of CdTB in ASFV-infected cells at 16 hpi by transmission electron microscopy (TEM). Cytoplasmic factories formed in the absence of CdTB contained the expected viral structures (envelope precursors and immature and mature icosahedral particles) (Fig. 4B). In contrast, those that developed after treatment with this inhibitor contained higher ratios of nonicosahedral envelope precursors and immature viral particles and few mature icosahedral viral particles. Consistent with the data from confocal microscopy, an increment in viral factory size was also detected, and this increase appeared to be due to the accumulation of envelope precursors in CdTB-treated cells. Under these conditions, a smaller number of ribosomes were found compared to viral factories from control cells, where ribosomes often appear to be associated with immature or mature virus particles. After infection very few immature particles reach the plasma membrane to be released by budding (8a). However, in infected CdTB-treated cells, abundant immature or defective virus particles reached the plasma membrane. Virus budding occurs by means of filopodial extensions from the plasma membrane, apparently by actin polymerization (11, 37), but after Rho

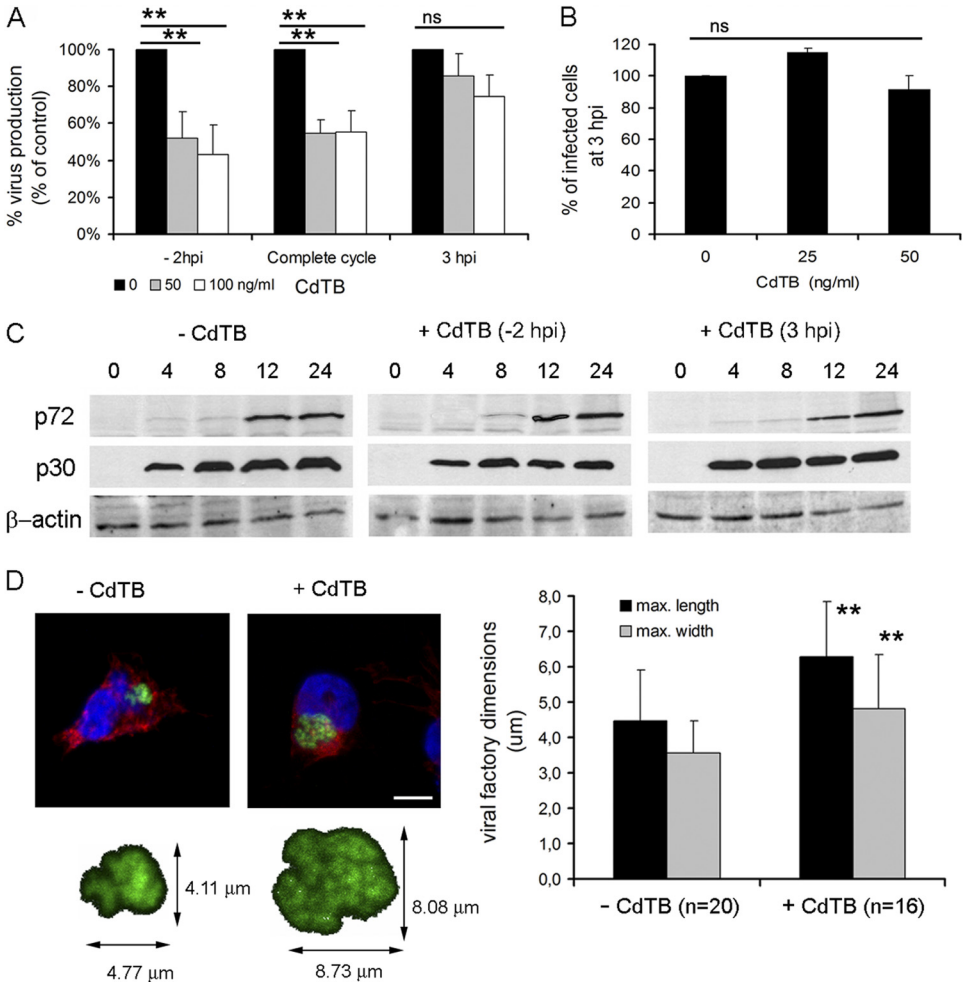

FIG 3 The downregulation of Rho GTPases impairs ASFV infection. Vero cells incubated for a range of times with increasing concentrations of toxin B from *Clostridium difficile* (CdTB) were infected with ASFV at 0.5 PFU/cell. (A) As described in the text, virus titers from infected cells at 24 hpi were determined by plaque assay and are shown as a percentage of untreated infected cells. (B) The number of infected cells at 3 hpi is represented as a percentage of untreated infected cells. The means and SD correspond to three independent experiments. Values that are significantly different from each other are indicated (**, $P < 0.01$; *, $P < 0.05$). (C) The expression of early (p30) and late (p72) viral proteins was analyzed at several time points during infection in cells treated with 100 ng of CdTB/ml 2 h prior to infection or 3 hpi and compared to untreated infected cells. β-Actin was used as a protein load control. (D) Vero cells were infected with B54GFP-2 in the presence or absence of CdTB and examined by confocal microscopy at 16 hpi. Viral factories from 16 to 20 cells were measured, and maximum dimensions are represented as means with the corresponding SD. A representative image is shown, where viral factories were detected by direct visualization of p54-EGFP (green). Nuclei (blue) and actin (red) were detected by Hoechst staining and anti-β actin antibody, respectively. Bar, 10 μm. Values significantly ($P < 0.01$) different from controls are indicated (**).

GTPases inactivation with CdTB no filopodia could be observed by TEM. In summary, these results indicate that early inhibition of Rho GTPase-mediated signaling with CdTB during the first stages of infection negatively affects virus progeny, virion maturation, and virus assembly site composition.

ASFV infection induces the activation of Rac1 GTPase in Vero cells. The requirement of Rho GTPases for efficient virus multiplication at early infection led us to explore the members of this family that are activated during ASFV entry. We specifically examined RhoA, Rac1, and Cdc42, the most extensively characterized members of the Rho GTPase family. All of these GTPases were inhibited by CdTB. RhoA, Rac1, and Cdc42 induction was monitored by an enzyme-linked immunosorbent assay (ELISA)-based assay (G-Lisa) at a range of times within first hour after virus inoculation in Vero cells (Fig. 5D), and the activation of Rac1 and Cdc42 could be also determined by an established affinity precipitation assay using GST-PBD, followed by immunoblot analysis (Fig. 5A to C). No activation of RhoA was observed by G-Lisa assay during the first hour after ASFV infection since active RhoA levels were similar to those obtained for mock-infected cells (Fig. 5D). Likewise, no activation of Cdc42 during first hour postinfection could be detected by G-Lisa and pulldown assay. In contrast, in the same conditions, a gradual increase in Rac1-GTP (the active form of Rac1) was observed during first 30 min of ASFV infection, with maximum activation at 25 min postinfection. At this time point, Rac1 was consistently activated ~3-fold over mock-infected cells (Fig. 5A and C). Interestingly, Rac1-GTP levels were restored to basal levels 5 min later, at 30 min postinfection. The total Rac1 in infected cells was not significantly modified during infection, thereby indicating the specificity of GTP activation. A Rac1-specific G-Lisa assay confirmed a Rac1 activation peak during the first 30 min of infection (Fig. 5D). These results support

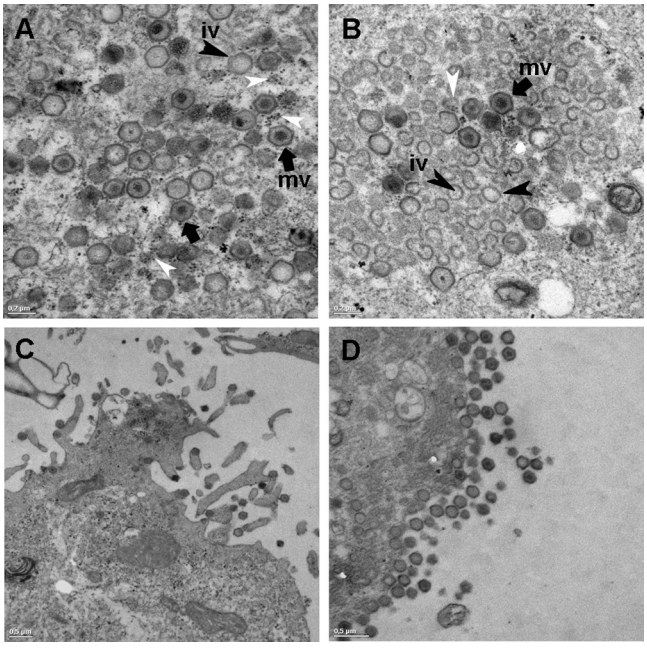

FIG 4 Electron microscopy analysis of ASF viral factory after inhibition of Rho GTPase-mediated signaling. Vero cells were infected with ASFV at 0.5 PFU/cell in the presence or absence of 50 ng of CdTB/ml and fixed at 16 hpi. (A) In the absence of CdTB, viral factories contained envelope precursors and abundant immature (iv, black arrowheads) and mature icosahedral particles (mv, arrows). (B) In contrast, viral factories formed in the presence of CdTB contained high amounts of envelope precursors and low numbers of both mature and immature icosahedral particles. (C) In the absence of CdTB, almost all viral particles that reached the plasma membrane were mature and were found with the characteristic filopodia in exocytosis. This observation contrasts with the abundant immature particles found at the cell membrane in the presence of CdTB and the absence of filopodia formation. (D). Scale bars: A and B, 0.2 μm; C and D, 0.5 μm. White arrowheads indicate ribosomes.

the hypothesis that Rac1 is the member of the Rho-GTPase family that is immediately activated after ASFV entry and that it is crucial for an efficient infection.

Effect of specific inhibition of Rac1 signaling on ASFV infection of Vero cells. To ascertain the specificity of Rac1 action during ASFV infection, we inhibited this GTPase, without affecting the other members of the Rho GTPase family. We used a chemical inhibitor, NSC23766, to prevent the specific activation of Rac1 and analyze impact on virus production (21). Cells were incubated with nontoxic doses of NSC23766 before ASFV infection, and virus progeny was examined at 24 hpi. Virus yields obtained after NSC23766 incubation decreased in a dose-dependent manner (Fig. 6A). Consistent with the CdTB experiments, this effect on virus yields was greater when the inhibitor was added to cells before infection. When we analyzed ASFV infectivity in Rac1-inhibited cells, we could observe a slight but significant decrease in the number of infected cells at 3 hpi compared to untreated control cells (Fig. 6B). Given that Rac1 activation occurred immediately after infection, we next analyzed by confocal microscopy the number of internalized virus particles in infected Vero cells 1 h after virus infection with highly purified ASFV at a high MOI and also their positions with respect to the host cell nucleus. Inhibition of geranylgeranylation with GGTI-286 did not modify the number of internalized virions (ranging between 19.5 and 21.2 PFU/cell). However, we observed a significant decrease in the number of virions exhibiting a perinuclear location at 1 hpi after GGTI-286 treatment.

Similarly, ASFV perinuclear localization, but not virion internalization, was affected after NSC23766 Rac1 inhibition, since the percentage of perinuclear virions was significantly reduced under these conditions (Fig. 6C). These results indicate that Rac1 is the member of Rho GTPase family whose activation after ASFV entry

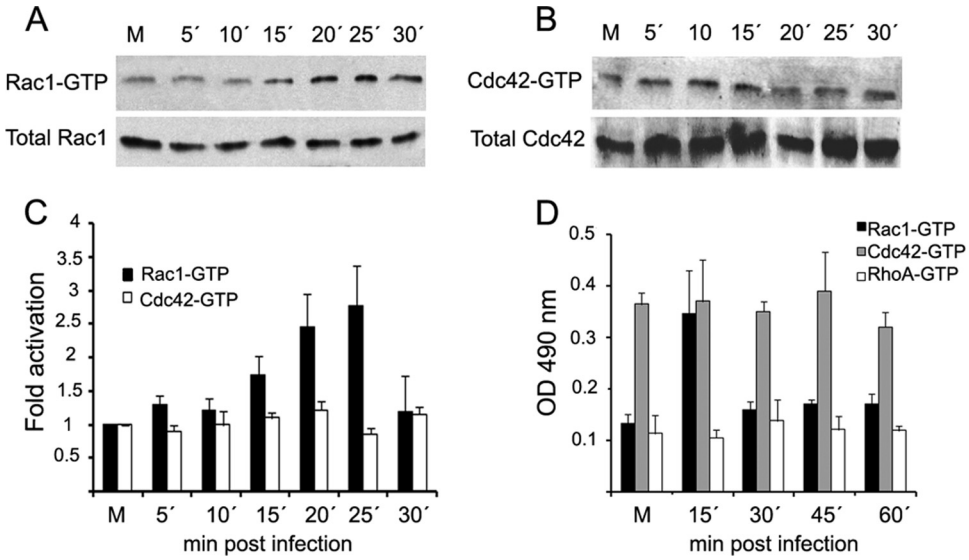

FIG 5 Rac1 is activated during early stages of ASFV infection. Equal amounts of Vero cell lysates from mock-infected cells (M) or ASFV-infected cells (5 PFU/cell) at various time points after infection were used to capture the GTP-bound form of Rac1 and Cdc42 by affinity precipitation with GST-PBD beads. The proteins captured by beads were analyzed by immunoblotting with anti-Rac1 antibody and anti-Cdc42 (top portions of panels A and B, respectively). The bottom portions of panels A and B show normalized cell lysates analyzed for total Rac1 as a protein load control. (C) Bands corresponding to GTP-bound forms of Rac1 and Cdc42 were quantified and normalized to values from total Rac1 and Cdc-42, respectively. The data obtained from mock-infected cells were considered to be activated 1-fold for comparison with infected cells. Representative images are shown from five independent pulldown assays. (D) Activation of Rac1, Cdc42, and RhoA was analyzed by an ELISA-based assay in infected Vero cells at the indicated time points within the first hour of infection. The GTP-bound forms of Rho GTPases were measured with an absorbance set at 490 nm. Each point represents the means ± the SD for three independent experiments.

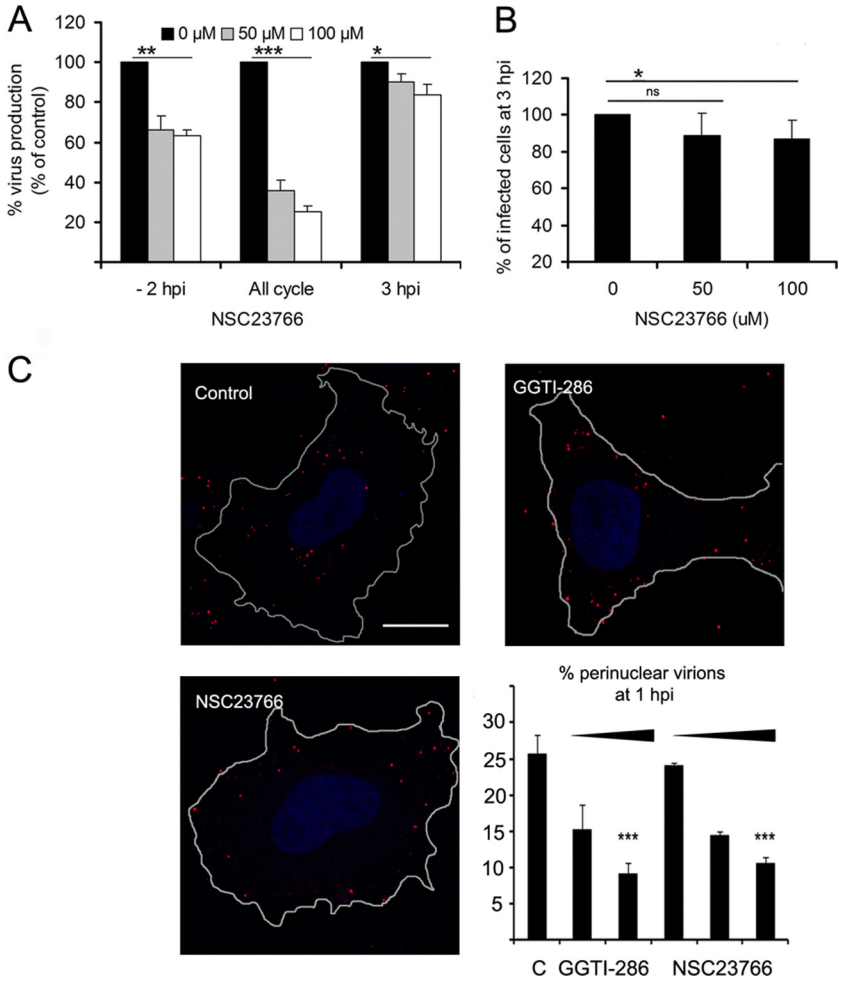

FIG 6 (A) Virus progeny at 24 hpi were determined by plaque assay from ASFV-infected cells in the presence of the specific Rac1 inhibitor NSC23766. Increasing, but nontoxic, concentrations of NSC23766 were added to cells before (−2 hpi), after (+3 hpi), or throughout infection. (B) The number of infected cells at 3 hpi in the presence of a range of concentrations of NSC23766 is shown as a percentage of control nontreated cells. (C) Virion distribution at 1 hpi in ASFV-infected Vero cells after incubation with increasing concentrations of GGTI-286 (10 and 30 μM) or NSC23766 (10, 50, and 100 μM) was examined. Representative confocal 0.1-μm sections from the z-axis are shown where virions were identified with mouse anti-p72 monoclonal antibody, followed by Alexa Fluor 594 anti-mouse IgG (red). Nuclei (blue) stained with Hoechst and cell contours are shown. Bar, 16 μm. A bar graph shows the percentage of virions exhibiting perinuclear localization. The data represent medians and SD from three independent experiments where 30 infected cells were analyzed in each case. A high MOI (>10 PFU/cell) was used. Each point represents the means ± the SD for three experiments. Values that are significantly different from each other are indicated (***, $P < 0.001$; **, $P < 0.01$; *, $P < 0.05$).

results relevant to reach perinuclear sites for an efficient virus multiplication. Also, Vero cells were transfected with plasmids encoding wild-type Rac1 (wt), dominant-negative Rac1 mutant (17N), or constitutively active Rac1 mutant (Q61L). After 24 h, the cells were mock infected or infected with a high MOI using highly purified ASFV. However, in transfected cells we were not able to find differences either in the number of internalized virus particles or in their positions with respect to the host cell nucleus at 1 hpi (data not shown).

ASFV infection induces microtubule hyperacetylation. Inhibition of Rac1 signaling negatively affected perinuclear virions localization but not entry itself, suggesting the involvement of Rac1 in following steps of infection immediately after ASFV entry. Early after ASFV entry into host cells, the microtubule network is essential for an efficient infection (3), and the acetylation/deacetylation balance of tubulin regulates microtubule dynamics (49), which is regulated by Rho GTPases. In addition, by using confocal microscopy, we detected the association of virions with acetylated microtubules during the first hour after virus inoculation in Vero cells (Fig. 7A). Since hyperacetylation is a quantitative indication of microtubules stabilization, we next analyzed tubulin acetylation levels from Vero cell extracts at a range of times postinfection by immunoblotting. Tubulin acetylation increased 2.5- to 4-fold from 15 to 30 min postinfection compared to mock-infected cells. At 45 min postinfection, tubulin acetylation levels showed a 2-fold increase, which was maintained for up 2 hpi and returned to basal levels by 3 hpi (Fig. 7B). In contrast, the levels of total α-tubulin remained unaltered. The inactivation of Rho GTPases with increasing concentrations of CdTB before infection restored tubulin acetylation levels to those obtained with mock-infected cell extracts (Fig. 7B). We specifically confirmed a reduction in tubulin acetylation levels in cells incubated with the geranylgeranylation inhibitor GGTI-286. Moreover, we observed similar re-

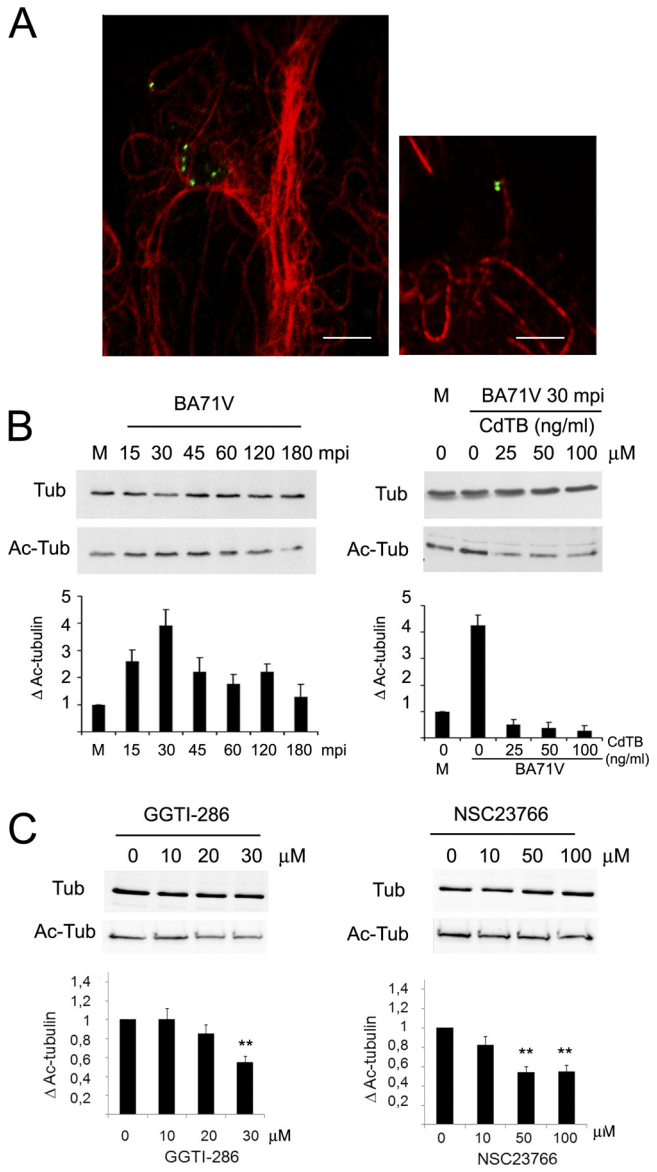

FIG 7 (A) Representative confocal microscopy image of ASFV-infected Vero cells at 30 min postinfection (mpi). ASF virions (green), detected by an antibody against viral protein pE120R, are coincident with acetylated microtubules (red). Bar, 10 μm. Total α-tubulin (Tub) and acetylated α-tubulin (Ac-Tub) levels were assessed by immunoblotting with specific antibodies from Vero cell extracts at a range of times during infection (B, left panel) and from infected Vero cells at 30 min in the presence of increasing concentrations of CdTB (B, right panel). (C) Similarly, acetylated tubulin levels were assessed from cell extracts after incubation for 2 h with increasing concentrations of GGTI-286 or NSC23766. In all cases, the band intensities were quantitated, and the acetylated tubulin in mock-infected or untreated Vero cells was considered as 1-fold for comparison with infected or inhibitor treated cells. Each bar represents the mean and SD corresponding to three independent experiments. Values that are significantly different from each other are indicated (***, $P < 0.001$; **, $P < 0.01$).

ductions in tubulin acetylation levels after inhibition of Rac1 signaling with increasing concentrations of specific Rac1 inhibitor NSC23766 (Fig. 7C). Taken together, these data suggest that Rac1 GTPase contributes to the microtubule hyperacetylation induced by ASFV during the early stages of Vero cell infection.

DISCUSSION

In this work, we have described the antiviral effects of statins on ASFV and how these are likely mediated by inhibition of prenylation of Rho GTPases. The initial results reported here demonstrate that lipid posttranslational modifications of host cell factors are important for an efficient infection and could participate in various stages of ASFV infection. We found that statins negatively affected virus production and infectivity (understood as infected cells at 3 hpi expressing ASFV early proteins), and this effect was fully reversed by the addition of immediate precursor Mev, whereas the addition of isoprenoid GGPP only restored virus infectivity. Specific inhibition of the prenyltransferases FTase-I and GGTase-I revealed that the incorporation of FPP is required during early stages of ASFV infection and that it is relevant for the subsequent development of infection. However, geranylation also participates in diverse steps of ASFV infection. The reduction of virus progeny when geranylation was inhibited after virus entry suggests that intact pools of GGPP or geranylated proteins during a later stage of ASFV infection are also crucial for correct viral replication. In this regard, ASFV encodes a *trans*-prenyltransferase (open reading frame *B318L*) that catalyzes the condensation of farnesyl diphosphate and isopentenyl diphosphate to GGPP and longer chain prenyl diphosphates (1, 2). *B318L* is an essential gene whose expression occurs late during virus infection, and its protein remains associated with precursor viral membranes derived from the endoplasmic reticulum at the viral assembly sites. These features are consistent with the hypothesis that GGPP synthesized by *B318L* serves as a substrate for the prenylation of cellular or viral proteins and that this posttranslational modification is required during virus replication and morphogenesis as described for hepatitis δ virus and murine leukemia virus (23, 34, 39, 49).

Isoprenoid intermediates are crucial for multiple cellular functions, such as the posttranslational modifications (prenylation) of a large variety of proteins, among which the small GTP-binding proteins Ras and Ras-like proteins, such as Rho, Rap, Rac, and Rab. Since prenylation of Rab GTPases is dependent on GGTase II, which is not affected by the inhibitor GGTI-286, the main focus of the present study was the Rho GTPase family. These are key regulators of the cell cytoskeleton, cell cycle, gene expression, and vesicle trafficking (19, 51) and are involved in the entry of diverse viruses into the host cell (14, 42, 48, 52) but also in viral morphogenesis (27, 61), infection spreading (12), or virus-induced cell motility (61, 66). In this regard, a general inhibition of Rho GTPase-mediated signaling could affect simultaneously diverse and relevant cellular processes that may explain the abnormal viral factory size and extensive accumulation of envelope precursors and immature virions observed when ASFV infection takes place under these conditions. It has been reported that Rho GTPases also participate in the morphogenesis of diverse viruses. For instance, RhoA is activated during late stages of respiratory syncytial virus infection and is crucial for correct filamentous virion morphology (26). During late infection, the alphaherpesviruses HSV-2 or pseudorabies virus promote actin rearrangements, presumably by viral protein US3 regulation of RhoA, Cdc42, and Rac1 activity balance (20, 47). Our observations with TEM on late stages of ASFV infection revealed a severe decrease of filopodia after CdTB treatment, which could be explained by a general Rho GTPase-mediated signaling inhibition with consequences on cor-

tical actin barrier regulation. However, and given that a high number of immature virus particles are accumulated at the cell surface after CdTB treatment, we cannot rule out the possibility that mature ASFV particles were required for stimulating filopodia formation, as reported for vaccinia virus-induced actin tails that resemble filopodia (reviewed in reference 56).

Our data with CdTB indicated that cellular signaling pathways regulated by Rho GTPases are activated during early stages of ASFV infection; however, its inactivation did not affect virus infectivity. Moreover, virus internalization was not affected by geranylgeranylation inhibition, thus demonstrating that Rho GTPases are not essential for ASFV entry itself in Vero cells.

Among the most extensively characterized members of the Rho GTPase family, we have demonstrated that Rac1 is activated during the first 30 min of ASFV infection in Vero cells. Surprisingly, Cdc42, which may act as an upstream activator of Rac1, was not induced by ASFV infection, as deduced from pull-down and also ELISA-based assays. A similar situation, Rac1 but not Cdc42 activation, was also recently described during hepatitis B virus infection (59). Rac1 regulates a wide variety of cellular functions (8) and participates in the entry of the following viruses into the host cell: vaccinia virus (44), dengue virus (65), herpes simplex virus 1 (33, 50), group B coxsackieviruses (13), and hepatitis B virus (59), among others. Most of these viruses exploit macropinocytosis in some way in order to gain access to the host cell by means of membrane ruffling or blebbing, which requires Rac1 activation (45). However, this entry strategy does not appear to be followed by ASFV, which enters the host cell by dynamin- and clathrin-dependent endocytosis (31), since specific Rac1 inhibition by NSC23766 before virus addition did not affect virus internalization, thus indicating the absence of deficiencies in ASFV endocytosis.

Thus, Rac1 may participate in further steps of early infection, such as intracellular transport to replication sites. Indeed, microtubule network integrity during the initial stages of ASFV infection is critical for successful infection (3). Our results demonstrate that ASFV infection promotes early microtubule hyperacetylation, a hallmark of the preferential stabilization of these structures. This process may be regulated by Rho GTPases, since their inhibition prevented microtubule hyperacetylation. Adenovirus and Kaposi's sarcoma-associated herpesvirus also induce microtubule hyperacetylation during early infection of human foreskin fibroblast (HFF) cells by a RhoA- and Rac1-dependent mechanism (48, 64). However, in A549 cells, microtubule hyperacetylation induced by incoming adenovirus is mediated exclusively by a Rac1-dependent mechanism (63), as we observed for ASFV. We determined that maximal Rac1 activity during early ASFV infection is coincident with hyperacetylation of microtubules (around 30 min postinfection), and tubulin acetylation levels were reduced after inhibition of Rac1 signaling with increasing concentrations of specific inhibitor.

Moreover, our results showed that specific inhibition of Rac1-mediated signaling with NSC23766 impaired virion perinuclear localization but not viral entry itself. Similar results were obtained with geranylgeranyl inhibitor which is concordant with a Rac1-mediated signaling inhibition by GGTI-286, given that Rac1 undergoes geranylgeranylation at its C terminus, and this posttranslational modification has been previously associated with an increase in Rac1 GTP binding and activation (46). However, we did not find differences in Rac1 dominant-negative mutant transfected cells affecting either the number of internalized virions or their localization to perinuclear areas. A possible explanation is that the inhibition of Rac1 in Vero cells was not complete in this case and a minimal proportion of acetylated microtubules might be sufficient to facilitate the start of ASFV infection.

Our data suggest that Rac1 modulates the intracellular transport of ASFV by inducing microtubule acetylation. In this regard, microtubules and associated molecular motors have been previously shown to be critical for ASFV trafficking from entry to replication and assembly sites (3), and these results open up the possibility that Rho GTPases could constitute an early target for statins during ASFV infection, relevant for the development of novel strategies to the eradication of African swine fever.

ACKNOWLEDGMENTS

We thank Ole Gjoerup for the plasmids encoding wild-type, dominant-negative, and constitutively active forms of Rac1 fused to GFP. The construct expressing the GST-Rac1/Cdc42 binding domain of Pak1 was a generous gift from Keith Burridge.

This study was supported by grants from Consolider Program CSD2006-00007 and by AGL2009-09209 from the Spanish Ministry of Science and Innovation.

REFERENCES

1. **Alejo A, Andres G, Vinuela E, Salas ML.** 1999. The African swine fever virus prenyltransferase is an integral membrane trans-geranylgeranyl-diphosphate synthase. J. Biol. Chem. **274**:18033–18039.
2. **Alejo A, Yanez RJ, Rodriguez JM, Vinuela E, Salas ML.** 1997. African swine fever virus *trans*-prenyltransferase. J. Biol. Chem. **272**:9417–9423.
3. **Alonso C, et al.** 2001. African swine fever virus protein p54 interacts with the microtubular motor complex through direct binding to light-chain dynein. J. Virol. **75**:9819–9827.
4. **Arakawa Y, Cordeiro JV, Way M.** 2007. F11L-mediated inhibition of RhoA-mDia signaling stimulates microtubule dynamics during vaccinia virus infection. Cell Host Microbe **1**:213–226.
5. **Bagrodia S, Taylor SJ, Jordon KA, Van Aelst L, Cerione RA.** 1998. A novel regulator of p21-activated kinases. J. Biol. Chem. **273**:23633–23636.
6. **Bernardes C, Antonio A, Pedroso de Lima MC, Valdeira ML.** 1998. Cholesterol affects African swine fever virus infection. Biochim. Biophys. Acta **1393**:19–25.
7. **Bos JL, Rehmann H, Wittinghofer A.** 2007. GEFs and GAPs: critical elements in the control of small G proteins. Cell **129**:865–877.
8. **Bosco EE, Mulloy JC, Zheng Y.** 2009. Rac1 GTPase: a "Rac" of all trades. Cell. Mol. Life Sci. **66**:370–374.
8a. **Brookes SM, Dixon LK, Parkhouse RM.** 1996. Assembly of African swine fever virus: quantitative ultrastructural analysis in vitro and in vivo.Virology **224**:84–92.
9. **Bustelo XR, Sauzeau V, Berenjeno IM.** 2007. GTP-binding proteins of the Rho/Rac family: regulation, effectors and functions in vivo. Bioessays **29**:356–370.
10. **Carrascosa AL, del Val M, Santaren JF, Vinuela E.** 1985. Purification and properties of African swine fever virus. J. Virol. **54**:337–344.
11. **Carvalho ZG, De Matos AP, Rodrigues-Pousada C.** 1988. Association of African swine fever virus with the cytoskeleton. Virus Res. **11**:175–192.
12. **Cordeiro JV, et al.** 2009. F11-mediated inhibition of RhoA signaling enhances the spread of vaccinia virus in vitro and in vivo in an intranasal mouse model of infection. PLoS One **4**:e8506.
13. **Coyne CB, Shen L, Turner JR, Bergelson JM.** 2007. Coxsackievirus entry across epithelial tight junctions requires occludin and the small GTPases Rab34 and Rab5. Cell Host Microbe **2**:181–192.
14. **del Real G, et al.** 2004. Statins inhibit HIV-1 infection by down-regulating Rho activity. J. Exp. Med. **200**:541–547.
15. **de Rooij J, Bos JL.** 1997. Minimal Ras-binding domain of Raf1 can be used as an activation-specific probe for Ras. Oncogene **14**:623–625.
16. **Diebold BA, Fowler B, Lu J, Dinauer MC, Bokoch GM.** 2004. Antagonistic cross-talk between Rac and Cdc42 GTPases regulates generation of reactive oxygen species. J. Biol. Chem. **279**:28136–28142.
17. **Dixon LK, et al.** 2005. *Asfarviridae*, p 135–143. *In*Fauquet CM, et al. (ed),

Virus taxonomy: eighth report of the International Committee on Taxonomy of Viruses. Elsevier/Academic Press, London, England.
18. **Enjuanes L, Carrascosa AL, Moreno MA, Vinuela E.** 1976. Titration of African swine fever (ASF) virus. J. Gen. Virol. **32**:471–477.
19. **Etienne-Manneville S, Hall A.** 2002. Rho GTPases in cell biology. Nature **420**:629–635.
20. **Favoreel HW, Van Minnebruggen G, Adriaensen D, Nauwynck HJ.** 2005. Cytoskeletal rearrangements and cell extensions induced by the US3 kinase of an alphaherpesvirus are associated with enhanced spread. Proc. Natl. Acad. Sci. U. S. A. **102**:8990–8995.
21. **Gao Y, Dickerson JB, Guo F, Zheng J, Zheng Y.** 2004. Rational design and characterization of a Rac GTPase-specific small molecule inhibitor. Proc. Natl. Acad. Sci. U. S. A. **101**:7618–7623.
22. **Geraldes A, Valdeira ML.** 1985. Effect of chloroquine on African swine fever virus infection. J. Gen. Virol. **66**(Pt 5):1145–1148.
23. **Glenn JS, Watson JA, Havel CM, White JM.** 1992. Identification of a prenylation site in delta virus large antigen. Science **256**:1331–1333.
24. **Goldstein JL, Brown MS.** 1990. Regulation of the mevalonate pathway. Nature **343**:425–430.
25. **Gomez-Puertas P, et al.** 1995. Improvement of African swine fever virus neutralization assay using recombinant viruses expressing chromogenic marker genes. J. Virol. Methods **55**:271–279.
26. **Gower TL, et al.** 2005. RhoA signaling is required for respiratory syncytial virus-induced syncytium formation and filamentous virion morphology. J. Virol. **79**:5326–5336.
27. **Gower TL, Peeples ME, Collins PL, Graham BS.** 2001. RhoA is activated during respiratory syncytial virus infection. Virology **283**:188–196.
28. **Guijarro C, et al.** 1998. 3-Hydroxy-3-methylglutaryl coenzyme a reductase and isoprenylation inhibitors induce apoptosis of vascular smooth muscle cells in culture. Circ. Res. **83**:490–500.
29. **Heasman SJ, Ridley AJ.** 2008. Mammalian Rho GTPases: new insights into their functions from in vivo studies. Nat. Rev. Mol. Cell. Biol. **9**:690–701.
30. **Heath CM, Windsor M, Wileman T.** 2001. Aggresomes resemble sites specialized for virus assembly. J. Cell Biol. **153**:449–455.
31. **Hernaez B, Alonso C.** 2010. Dynamin- and clathrin-dependent endocytosis in African swine fever virus entry. J. Virol. **84**:2100–2109.
32. **Hernaez B, Escribano JM, Alonso C.** 2006. Visualization of the African swine fever virus infection in living cells by incorporation into the virus particle of green fluorescent protein-p54 membrane protein chimera. Virology **350**:1–14.
33. **Hoppe S, et al.** 2006. Early herpes simplex virus type 1 infection is dependent on regulated Rac1/Cdc42 signaling in epithelial MDCKII cells. J. Gen. Virol. **87**:3483–3494.
34. **Hwang SB, Lai MM.** 1993. Isoprenylation mediates direct protein-protein interactions between hepatitis large delta antigen and hepatitis B virus surface antigen. J. Virol. **67**:7659–7662.
35. **Jaffe AB, Hall A.** 2005. Rho GTPases: biochemistry and biology. Annu. Rev. Cell Dev. Biol. **21**:247–269.
36. **Jouvenet N, Monaghan P, Way M, Wileman T.** 2004. Transport of African swine fever virus from assembly sites to the plasma membrane is dependent on microtubules and conventional kinesin. J. Virol. **78**: 7990–8001.
37. **Jouvenet N, et al.** 2006. African swine fever virus induces filopodia-like projections at the plasma membrane. Cell Microbiol. **8**:1803–1811.
38. **King DP, et al.** 2003. Development of a TaqMan PCR assay with internal amplification control for the detection of African swine fever virus. J. Virol. Methods **107**:53–61.
39. **Lee CZ, Chen PJ, Lai MM, Chen DS.** 1994. Isoprenylation of large hepatitis delta antigen is necessary but not sufficient for hepatitis delta virus assembly. Virology **199**:169–175.
40. **Li E, Stupack D, Bokoch GM, Nemerow GR.** 1998. Adenovirus endocytosis requires actin cytoskeleton reorganization mediated by Rho family GTPases. J. Virol. **72**:8806–8812.
41. **Liao JK, Laufs U.** 2005. Pleiotropic effects of statins. Annu. Rev. Pharmacol. Toxicol. **45**:89–118.
42. **Locker JK, et al.** 2000. Entry of the two infectious forms of vaccinia virus at the plasma membrane is signaling-dependent for the IMV but not the EEV. Mol. Biol. Cell **11**:2497–2511.
43. **McTaggart SJ.** 2006. Isoprenylated proteins. Cell. Mol. Life Sci. **63**: 255–267.
44. **Mercer J, Helenius A.** 2010. Apoptotic mimicry: phosphatidylserine-mediated macropinocytosis of vaccinia virus. Ann. N. Y. Acad. Sci. **1209**: 49–55.
45. **Mercer J, Helenius A.** 2009. Virus entry by macropinocytosis. Nat. Cell Biol. **11**:510–520.
46. **Michaelson D, et al.** 2001. Differential localization of Rho GTPases in live cells: regulation by hypervariable regions and RhoGDI binding. J. Cell Biol. **152**:111–126.
47. **Murata T, Goshima F, Daikoku T, Takakuwa H, Nishiyama Y.** 2000. Expression of herpes simplex virus type 2 US3 affects the Cdc42/Rac pathway and attenuates c-Jun N-terminal kinase activation. Genes Cells **5**:1017–1027.
48. **Naranatt PP, Krishnan HH, Smith MS, Chandran B.** 2005. Kaposi's sarcoma-associated herpesvirus modulates microtubule dynamics via RhoA-GTP-diaphanous 2 signaling and utilizes the dynein motors to deliver its DNA to the nucleus. J. Virol. **79**:1191–1206.
49. **Overmeyer JH, Maltese WA.** 1992. Isoprenoid requirement for intracellular transport and processing of murine leukemia virus envelope protein. J. Biol. Chem. **267**:22686–22692.
50. **Petermann P, Haase I, Knebel-Morsdorf D.** 2009. Impact of Rac1 and Cdc42 signaling during early herpes simplex virus type 1 infection of keratinocytes. J. Virol. **83**:9759–9772.
51. **Qualmann B, Mellor H.** 2003. Regulation of endocytic traffic by Rho GTPases. Biochem. J. **371**:233–241.
52. **Quinn K, et al.** 2009. Rho GTPases modulate entry of Ebola virus and vesicular stomatitis virus pseudotyped vectors. J. Virol. **83**:10176–10186.
53. **Ridley AJ.** 2001. Rho family proteins: coordinating cell responses. Trends Cell Biol. **11**:471–477.
54. **Rodriguez JM, Garcia-Escudero R, Salas ML, Andres G.** 2004. African swine fever virus structural protein p54 is essential for the recruitment of envelope precursors to assembly sites. J. Virol. **78**:4299–4313.
55. **Sander EE, et al.** 1998. Matrix-dependent Tiam1/Rac signaling in epithelial cells promotes either cell-cell adhesion or cell migration and is regulated by phosphatidylinositol 3-kinase. J. Cell Biol. **143**:1385–1398.
56. **Smith GL, Vanderplasschen A, Law M.** 2002. The formation and function of extracellular enveloped vaccinia virus. J. Gen. Virol. **83**:2915–2931.
57. **Stefanovic S, Windsor M, Nagata KI, Inagaki M, Wileman T.** 2005. Vimentin rearrangement during African swine fever virus infection involves retrograde transport along microtubules and phosphorylation of vimentin by calcium calmodulin kinase II. J. Virol. **79**:11766–11775.
58. **Subauste MC, et al.** 2000. Rho family proteins modulate rapid apoptosis induced by cytotoxic T lymphocytes and Fas. J. Biol. Chem. **275**: 9725–9733.
59. **Tan TL, et al.** 2008. Rac1 GTPase is activated by hepatitis B virus replication: involvement of HBX. Biochim. Biophys. Acta **1783**:360–374.
60. **Valdeira ML, Bernardes C, Cruz B, Geraldes A.** 1998. Entry of African swine fever virus into Vero cells and uncoating. Vet. Microbiol. **60**: 131–140.
61. **Valderrama F, Cordeiro JV, Schleich S, Frischknecht F, Way M.** 2006. Vaccinia virus-induced cell motility requires F11L-mediated inhibition of RhoA signaling. Science **311**:377–381.
62. **Van Aelst L, D'Souza-Schorey C.** 1997. Rho GTPases and signaling networks. Genes Dev. **11**:2295–2322.
63. **Warren JC, Cassimeris L.** 2007. The contributions of microtubule stability and dynamic instability to adenovirus nuclear localization efficiency. Cell Motil. Cytoskeleton **64**:675–689.
64. **Warren JC, Rutkowski A, Cassimeris L.** 2006. Infection with replication-deficient adenovirus induces changes in the dynamic instability of host cell microtubules. Mol. Biol. Cell **17**:3557–3568.
65. **Zamudio-Meza H, Castillo-Alvarez A, Gonzalez-Bonilla C, Meza I.** 2009. Cross-talk between Rac1 and Cdc42 GTPases regulates formation of filopodia required for dengue virus type 2 entry into HMEC-1 cells. J. Gen. Virol. **90**:2902–2911.
66. **Zwilling J, Sliva K, Schwantes A, Schnierle B, Sutter G.** 2010. Functional F11L and K1L genes in modified vaccinia virus Ankara restore virus-induced cell motility but not growth in human and murine cells. Virology **404**:231–239.